

## Hydrogen Peroxide Treated Desiccated Coconut Waste as a Biosorbent in Malachite Green Removal from Aqueous Solutions

Shuhaila Mohd Hussin<sup>1</sup>, Waheeba Ahmed Al-Amrani<sup>2</sup>, Faiz Bukhari Mohd Suah<sup>3</sup>, La Harimu<sup>4</sup>, Megat Ahmad Kamal Megat Hanafiah<sup>1\*</sup>

<sup>1</sup> Faculty of Applied Sciences, Universiti Teknologi MARA Pahang, 26400, Jengka, Pahang, Malaysia

<sup>2</sup> Department of Chemistry, College of Science, Ibb University, Ibb, Yemen

<sup>3</sup> School of Chemical Sciences, Universiti Sains Malaysia, 11800, Minden, Penang, Malaysia

<sup>4</sup> Department of Chemistry Education, Faculty of Teacher Training and Education, Halu Oleo University, Kendari, Sulawesi Tenggara, Indonesia

\* Corresponding author's e-mail: makmh@uitm.edu.my

### ABSTRACT

Malachite green (MG), commonly employed in the textile and dyeing sectors, is a prevalent and enduring contaminant found in wastewater and the environment. Its presence poses harmful effects to humans and aquatic organisms. This work utilised hydrogen peroxide-treated desiccated coconut waste (HPDCW) to remove MG from an aqueous solution. The HPDCW underwent characterisation utilising FTIR, SEM-EDX,  $\text{pH}_{\text{slurry}}$ , and  $\text{pH}_{\text{pzc}}$ . Based on the results obtained, it was found that HPDCW recorded a biosorption capacity of 211.88 mg/g, attained at a temperature of 302 K, a pH of 9, a contact period of 5 min, and a dosage of 0.02 g. MG biosorption rates accurately followed the pseudo-second-order kinetic model, while the equilibrium data presented a step-shaped isotherm model. The relatively small percentages of MG desorption observed when using distilled water and HCl (0.01 and 0.02 M) indicate that electrostatic interaction is one of the mechanisms responsible for the interaction between MG and HPDCW. There is also a possibility of the involvement of hydrogen bonding and  $\pi$ - $\pi$  interactions.

**Keywords:** biosorption, desiccated coconut, isotherm, kinetic, malachite green.

### INTRODUCTION

The escalating worldwide apprehension regarding water pollution caused by both inorganic and organic substances is primarily driven by the potential health risks and environmental consequences associated with it. Within this group of organic chemicals, synthetic dyes have emerged as significant pollutants as a result of the substantial release of wastewater with elevated dye concentrations from various industrial sectors (Al-Amrani et al., 2022; Zhang et al., 2021). Malachite green (MG) is frequently employed for the purpose of colouring various materials, including silk, wool, leather, cotton, distilleries, paper, and jute. Aquaculture employs it as an antiseptic, antiparasitic agent, and fungicide. Although it is harmful, this dye is nevertheless used in multiple

nations, mostly due to its easy availability, high efficacy and low cost. Recent findings indicate that when animals consume this dye orally, it can lead to toxicity, carcinogenicity, mutagenicity, and teratogenicity (He et al., 2023; Zainon et al., 2023). In humans, inhalation of MG can result in respiratory system damage and perhaps lead to infertility (Azaman et al., 2018). Hence, it is imperative to employ simple yet efficient technology for the treatment of dye wastewater prior to its discharge into natural bodies of water.

Biosorption is a versatile process that can effectively separate various substances. It offers economic advantages, is environmentally sustainable, and is compatible with biological systems. Additionally, it is capable of efficiently eliminating synthetic colours from wastewater (Ganiyu et al., 2023; Umeh et al., 2023). Various research

endeavours have utilised bioresources, specifically lignocellulosic materials, as biosorbents for the purpose of eliminating dyes. These biosorbents are not only cost-effective but also readily accessible locally (Prasad et al., 2023; Somsiripan & Sangwichien, 2023; Song et al., 2023; Widiarytiasari Prihatdini et al., 2023). Coconuts (*Cocos nucifera* L.) are Arecaceae palm trees with several applications (Chong & Tam, 2020). The species is predominantly cultivated along the coastal areas of Peninsular Malaysia, covering an area of 142,000 hectares. Consequently, a significant quantity of solid waste in the form of husk fibres and shells is generated on a yearly basis. Typically, the surplus is whichever is leftward to decompose or utilised as a combustible fuel, resulting in significant environmental disruption (Bello & Ahmad, 2012; Saikia et al., 2022). Enhancing coconuts to serve as adsorptive material in the treatment of municipal and industrial effluents or water purification will enhance the worth of these agricultural commodities and contribute to the reduction of waste disposal expenses.

Coconut husk ash (CHA) was utilised as a substrate for CoAl layered double hydroxide (LDH) and employed in the MG removal from aqueous solutions. The findings demonstrated that the CHA/CoAl-LDH composite exhibited a remarkable removal efficacy of 98.16% with a maximal Langmuir biosorption capacity of 666.4 mg/g when administered at a biosorbent dose of 0.015 g, with a preliminary MG concentration of 100 mg/L and a pH of 10 (Saikia et al., 2022). The discarded coconut fibres were processed and converted into cellulose-based aerogels using sodium hydroxide (NaOH) and hydrogen peroxide ( $H_2O_2$ ). These aerogels were then utilised to eliminate methylene blue (MB) from the water that contained it. The synthesised aerogels exhibit a low bulk of 0.034–0.063 g/cm<sup>3</sup> with a consistent porosity ranging from 96.30% to 98.32%. Moreover, they have exceptional biosorption capabilities for MB, with a biosorption capability of 625 mg/g, which is three times greater than that of uncarbonated aerogels (Nguyen et al., 2022). In another study, coconut shell activated carbon (CSAC) was utilised with great efficacy for removing MG. The relationship between the MG molecule and CSAC biosorbent was affected by the solution pH, resulting in a biosorption capacity of 61.83 mg/g at a temperature of 303 K (Azaman et al., 2018). Bello & Ahmad (2012) employed coconut shell-based activated carbon (CSAC) in batch studies to eliminate MG. The highest efficiency in removing

MG was achieved at a pH of 8.0 or above, with a maximum biosorption capacity of 187.43 mg/g at a temperature of 303 K. Nevertheless, the potential of using hydrogen peroxide to treat desiccated coconut waste (DCW) for adsorbing MG has not been studied.

In this work, DCW was subjected to hexane washing before being treated with hydrogen peroxide and applied for MG removal from synthetic wastewater. The biosorbent underwent characterisation using spectroscopic and quantitative tests. The biosorption of MG onto the biosorbent was examined under several experimental settings, such as varying pH levels, initial MG concentrations, and dosages.

## MATERIALS AND METHODS

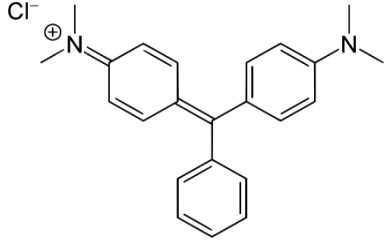
### Preparation of biosorbent

Raw DCW was bought from a local market in Jengka, Malaysia and underwent thorough rinsing and pressing with distilled water to remove the coconut milk. Subsequently, it was subjected to drying at a temperature of 80°C overnight. The DCW then underwent a pretreatment process involving the combination of hexane at a weight-to-volume ratio of 1:10. The mixture was left overnight to remove the fat content, filtered and dehydrated in the oven at 80 °C for 24 h. DCW was then subjected to a size reduction process, wherein it was crushed into fine particles ranging in size from 150 to 250 µm. Then, 1.0 g of DCW was brought into contact with 100 mL of  $H_2O_2$  (15%, v/v) heated at 50°C. After undergoing an hour of agitation, the resulting samples underwent a sequence of steps, including rinsing with distilled water, filtration, and drying at 80 °C for 24 h.

### Preparation of MG solution

The MG biosorption tests were performed employing a water-based solution of MG dye (99% purity) provided by R&M Chemicals, Malaysia. To prepare the experimental solution, 1000 mg/L MG standard solution was initially formulated utilising 1 L of distilled water. This solution was subsequently subjected to appropriate dilution procedures to attain the desired concentration of MG dye for the experimental trials. Detailed insights into the MG molecular structure and properties are comprehensively outlined in Table 1.

**Table 1.** Physiognomies of MG accompanied by its molecular structure

Physiognomies	MG	Molecular structure
Abbreviation	MG	
Type	Cationic dye	
Molecular weight	364.91 g/mol	
Chemical formula	C <sub>23</sub> H <sub>25</sub> N <sub>2</sub> Cl	
Parent Compound	CID 11295 (MG cation)	
Common Synonyms	China Green, MG 569-64-2, Basic Green 4, MG chloride.	
Appearance	In water solutions: Blue-green Metallic lustre with green crystals.	

### Characterisation of DCW and HPDCW

Employing an FTIR spectrophotometer (PerkinElmer, Spectrum 100, USA), the surface functional groups inherent to DCW, HPDCW, and MG-laden HPDCW were conclusively ascertained. The spectral analysis spanned the range of 4000 to 600 cm<sup>-1</sup>. Additionally, to examine the surface morphology of DCW and HPDCW, SEM coupled with EDX (Oxford Instrument, UK) was utilised. To determine surface charge using the pH at the point of zero charge (pH<sub>pzc</sub>) approach, a systematic evaluation of HPDCW was conducted as follows: Solutions comprising 50 mL of 0.01 M NaCl, exhibiting an initial pH (pH<sub>i</sub>) spanning from 3 to 9, were meticulously prepared. Subsequently, 0.50 g of HPDCW was immersed in these NaCl solutions for 24 h. The post-incubation stage encompassed the measurement of the final pH (pH<sub>f</sub>) in the supernatant post-filtration. The critical pH value in the ΔpH (pH<sub>f</sub> – pH<sub>i</sub>) versus pH<sub>i</sub> plot, where the curve meets the pH<sub>i</sub> axis, clearly marked the pH<sub>pzc</sub> of HPDCW. In addition, the slurry pH (pH<sub>slurry</sub>) was measured by immersing 0.50 g of DCW and HPDCW in 50 mL of distilled water in separate conical flasks. The mixture was allowed to sit at ambient temperature overnight before undergoing filtration using a Whatman filter paper (No. 42), and the pH resulting from the filtered solution was evaluated using a pH meter.

### Malachite green batch biosorption studies

The MG solution (50 mL) was sourced from the stock solution, and batch biosorption experiments were undertaken using 250 mL Erlenmeyer flasks. These flasks were placed on a 10-point magnetic stirrer operating at 300 rpm. The objective was to assess the impact

of varying quantities of HPDCW and solution pH on its biosorption efficacy for a 10 mg/L MG dye solution at 29 °C (room temperature). This assessment involved altering the pH of the MG solutions within 3 to 9. For dosage effect, HPDCW weight ranged from 0.02 to 0.10 g was applied, and the interaction time was fixed at 60 min. The pH adjustments were meticulously executed using a pH meter (Eutech Instruments pH 510, Singapore), and for this purpose, controlled additions of 0.10 M HCl or NaOH were introduced to each experimental setting. Additionally, kinetic investigations were conducted. For this purpose, 50 mL of MG solutions and 0.02 g of HPDCW were mixed at pH 9, encompassing different initial MG concentrations (10–30 mg/L). These mixtures were observed at certain time intermissions. Isotherm steadiness tests were conducted by the addition of 0.02 g of HPDCW into 50 mL of the investigated dye solution at pH 9. The initial MG concentrations (10–200 mg/L) were spanned at 60 min. To quantify the MG concentrations, a double-beam UV/Vis spectrophotometer (UV-1800, Shimadzu, Japan) was employed through measurements taken at a wavelength of 617 nm (λ<sub>max</sub>). The amount of MG adsorbed on HPDCW was calculated by means of Eq. (1), while the removal percentage was determined by Eq. (2):

$$q_e = \frac{(C_0 - C_e) \times V}{m} \quad (1)$$

$$\% \text{ Removal} = \frac{C_0 - C_e}{C_0} \times 100 \quad (2)$$

where:  $q_e$  is the amount of MG adsorbed,  $C_0$  is the initial MG concentration,  $C_e$  is MG equilibrium concentration,  $m$  is HPDCW dosage, and  $V$  is MG volume.

It is important to underscore that the biosorption experiments were duplicated, and the reported outcomes represent the averaged results.

### Desorption studies

Commencing the biosorption process of MG solutions, a measured volume of 50 mL from the 10 mg/L MG solutions was introduced into a 250 mL Erlenmeyer flask. Subsequently, an exact amount of 0.02 g of HPDCW was introduced, and the mixture was subjected to 1 h of agitation at 29 °C. After this phase, the solutions were filtered, followed by a UV-visible spectrophotometer analysis. The biosorbent was dried for 2 h in an 80 °C oven. The desorption protocol encompassed using distilled water and HCl solutions at different concentrations of 0.01 M and 0.02 M. In this process, 50 mL of each of the solutions mentioned above was transferred into 250 ml Erlenmeyer flasks. Subsequently, the previously dried HPDCW was introduced to each flask, and the contents were stirred for 1 h. The ensuing mixture was again subjected to filtration, and the resultant solution was subjected to scrutiny employing a UV-visible spectrophotometer. The percentage of MG desorbed was estimated using Eq. (3):

$$\text{Desorption efficiency (\%)} = \frac{\text{MG conc. after elution (mg/L)}}{\text{MG conc. before elution (mg/L)}} \times 100 \quad (3)$$

### Statistical analysis

To better match the investigational results toward the intended models, a non-linear regression assessment of the kinetic models was performed using the Solver add-in, Microsoft Excel. The assessment of the fitness level was conducted through the utilisation of statistical measures such as the determination constant ( $R^2$ ) then the non-linear chi-square ( $\chi^2$ ). The statistical properties were calculated utilising the subsequent mathematical equations:

$$R^2 = \frac{\sum(q_{e,calc,i} - q_{e,exp,i})^2}{\sum(q_{e,calc,i} - q_{e,exp,avg})^2 - \sum(q_{e,calc,i} - q_{e,exp,i})^2} \quad (4)$$

$$\chi^2 = \sum_{i=1}^N \left| \frac{(q_{e,exp,i} - q_{e,calc,i})^2}{q_{e,exp,i}} \right| \quad (5)$$

where  $q_{e,calc,i}$ ,  $q_{e,exp,i}$ , along with  $q_{e,exp,avg}$  are the model-premeditated and empirically observed biosorption capacity on HPDCW at any observation  $i$ , respectively,  $N$  represents the observation number.

## RESULTS AND DISCUSSION

### Biosorbent characterisation

Figure 1 displays the FTIR bands of raw DCW, HPDCW, and MG-laden HPDCW. The spectra of DCW, HPDCW, and MG-laden HPDCW did not exhibit any notable differences, except for the existence of a new peak at 1518  $\text{cm}^{-1}$  in the spectrum of MG-laden HPDCW. The spectra exhibit a broad peak at about 3356  $\text{cm}^{-1}$ , suggesting the existence of hydroxyl, carboxylic, and amine functional sets in cellulose and lignin (Azaman et al., 2018; Khalid et al., 2022). Furthermore, the C-H groups derived from cellulose groups are found within the range of 2854 to 2923  $\text{cm}^{-1}$ . The distinct peaks observed at 1744 and 1456  $\text{cm}^{-1}$  provide evidence for the existence of carboxylic acid functional groups. The bands seen at 1645 and 1643  $\text{cm}^{-1}$  represent the C=O functional group present in DCW and HPDCW, respectively. The existence of C-N from amino groups is indicated by the peak near 1242  $\text{cm}^{-1}$ . The band observed at around 1147  $\text{cm}^{-1}$  corresponds to the stretching of C-O or C-S, which are often present in alcohols, amino acids, ethers and esters (Piriya et al., 2023). The spectral range from 900 to 700  $\text{cm}^{-1}$  exhibits bands associated with aromatic compounds, namely the bending of out-of-plane C-H bonds through varying levels of replacement. Similar findings were documented while employing alternative biosorbents (Azaman et al., 2018; Bello & Ahmad, 2012; Zainon et al., 2023). The biosorption of MG onto HPDCW resulted in a decrease in the percentage of transmittance of the C=O functional group at 1744  $\text{cm}^{-1}$  and the appearance of a weak peak at 1518  $\text{cm}^{-1}$ , representing the C=N of MG. This proposes that amine and carboxylic groups play a key role in the biosorption process. Furthermore, the newly observed peak at 1518  $\text{cm}^{-1}$  can be associated with conjugated hydrogen-linked carboxyl groups with MG (Bello & Ahmad, 2012). The FTIR analysis reveals that both DCW and HPDCW include a significant amount of carboxyl, hydroxyl, amine, and aromatic groups. The MG biosorption on the HPDCW was facilitated through the interaction between the amine and -OH groups, which form hydrogen bonds or electrostatic interactions with the adsorbed MG molecules. Other weak intermolecular forces involved between HPDCW and MG, such as  $n-\pi$  and  $\pi-\pi$ , could not be ruled out. Figure 2 displays SEM and EDX images of the raw DCW, HPDCW, and MG-laden HPDCW. The

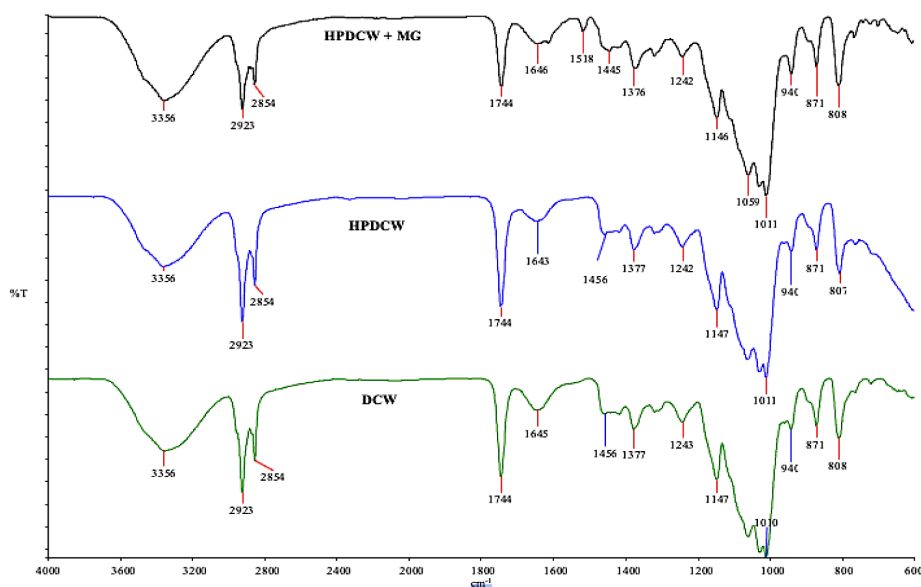


**Figure 1.** Spectra of FTIR of raw DCW, HPDCW, along with MG-laden HPDCW

surface texture of DCW exhibited a significant disparity prior to and subsequent to the treatment. The existence of hemicellulose and lignin in the raw DCW gives it a distinct morphological appearance, characterised by a hard, caves-like, and uneven surface (Figure 2A). However, when DCW is pretreated with hexane and  $H_2O_2$ , the lignin, oil, and fats are eliminated, leading to a spongy structure with pores (Figure 2C). This pretreatment not only increases the inner surface zone but also endorses the development of the pore, which is reliable with the research by Zainon Abidin et al. (2023). Furthermore, Figure 2D demonstrates that the oxygen content (O) of HPDCW is greater than that of DCW, as depicted in Figure 2B. The DCW has carbon (C) as the main component, accounting for 61.30% (by weight), whereas HPDCW contains 57.76% carbon. These observations suggest the successful oxidation process of the hydroxyl groups on the DCW surface to carboxylic groups using  $H_2O_2$  solution. After MG biosorption, the surface of MG-laden HPDCW proves that it has been roofed with a film of MG dye, as confirmed by the oxygen content decreases, as presented in Figure 2F, due to the binding between the hydroxyl groups in HPDCW and MG.

The  $pH_{slurry}$  refers to the pH value of a biosorbent, indicating its level of acidity or basicity. The  $pH_{pzc}$  refers to the pH level at which the amount of negative charges on the biosorbent surface is equivalent to the number of positive charges (Hanafiah et al., 2022). The pH values of the slurry are 6.44 and 4.88 for DCW and HPDCW, respectively. The

$pH_{pzc}$  value for HPDCW is 5.7, as shown in Figure 3. The surface properties of DCW and HPDCW biosorbent were determined to be acidic based on both the  $pH_{slurry}$  and  $pH_{pzc}$ . This indicates that the alteration has effectively altered the surface characteristics of the HPDCW. The decreased  $pH_{slurry}$  value of the HPDCW suggests an increase in the concentration of carboxylic acid groups following treatment with  $H_2O_2$ . When the pH is greater than the  $pH_{pzc}$ , the HPDCW surface will acquire a stronger negative charge. As a result, the MG biosorption would be favoured.

## Malachite green biosorption tests

### Impact of MG solution pH

The efficacy of the biosorption process can be greatly influenced by the MG solution pH. It regulates the charge of the biosorbent surface, impacts the chemistry of the dye, breaks apart functional groups of the biosorbent on the dynamic sites, and can ionise the molecules being adsorbed in the solution (Al-Amrani et al., 2022). Hence, Figure 4 visually represents the impact of varying initial pH of the MG solution on the biosorption process. The results clearly show that increasing the pH from 3.0 to 9.0 caused a simultaneous upsurge in the biosorption capacity. This is because of the electrostatic attraction among the positively charged MG and the negatively charged  $COO^-$  on the HPDCW surface. The decline in MG biosorption at pH levels below 7 can be ascribed to the loading of  $H_3O^+$  ions on the HPDCW surface. This outcome is consistent with

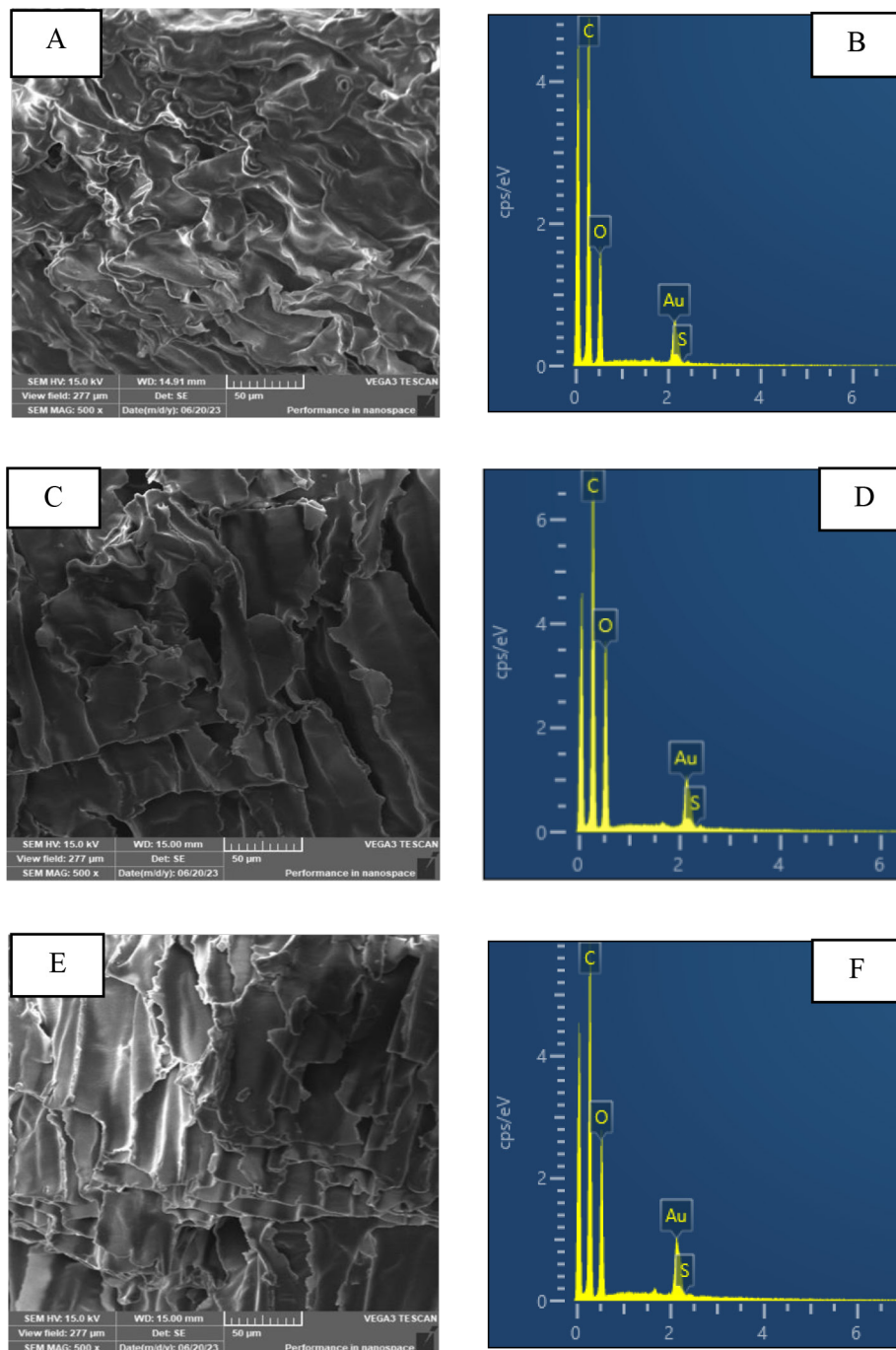


**Figure 2.** Images of SEM (amplification = 500X) and EDX of (A) raw DCW, (C) HPDCW, and (E) MG-laden HPDCW

prior analogous biosorption investigations (Azaman et al., 2018; Saikia et al., 2022; Zainon et al., 2023). Consequently, isotherm and kinetics studies were carried out on the MG solution at a pH of 9.

#### *Impact of HPDCW dosage*

The dosage of biosorbent is crucial for decisive biosorption capability since the biosorbent quantity introduced into the solution directly affects the

number of binding sites accessible for biosorption. Similarly, the removal ratio is significant as it reflects the effectiveness of the biosorbent in removing the target substance (Al-Amrani et al., 2022). Figure 5 demonstrates the impact of several dosages of HPDCW, ranging from 0.02 g to 0.10 g, on the elimination of MG with 10 mg/L from water solutions at pH 9 over 60 min. Significantly, it is evident that raising the dosage of HPDCW from 0.02 to 0.10 g resulted in an increase in the MG elimination in

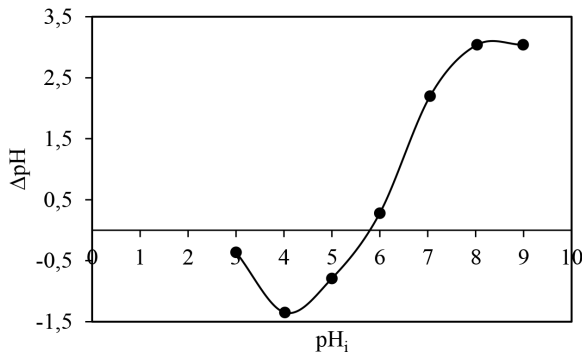


Figure 3. Value of  $pH_{pzc}$  of HPDCW

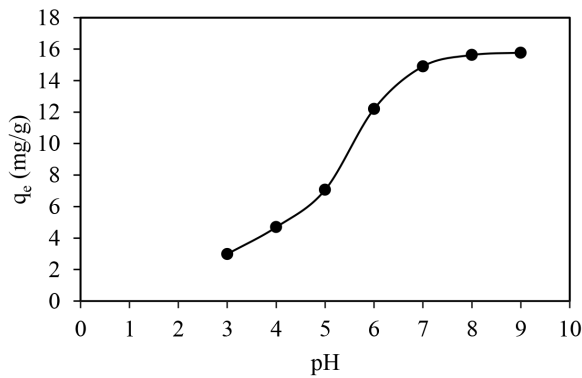


Figure 4. The impact of solution pH on the biosorption behaviour of MG at a concentration of 10 mg/L, HPDCW dosage of 0.02 g, 300 rpm, and 29°C

the bulk solution from 80.89% to 89.38%, although simultaneously reducing the capability of MG biosorption from 22 to 4 mg/g. The upsurge percentage of MG biosorption may be ascribed to an elevation in the accessible, energetic sites for MG biosorption. In contrast, the decrease in MG biosorption ability may be because of the aggregation or overlapping

of biosorption places at larger biosorbent dosages and the increase of unsaturated surface area for adsorbate. Therefore, subsequent investigations on kinetics and isotherms were conducted using 0.02 g of HPDCW. The results of other biosorption investigations were consistent with these observations (Lemos et al., 2023; Zainon et al., 2023).

### Biosorption kinetic studies

The impact of contact time on the MG biosorption using the HPDCW biosorbent is depicted in Figure 6. The biosorption capacity of HPDCW increases as the contact duration increases and reaches equilibrium within 5 min for all initial concentrations. Comprehending the kinetics of biosorption is crucial for identifying the optimal parameters for a batch operation on a big scale (Musah et al., 2022; Revellame et al., 2020). To examine the kinetics of MG biosorption using HPDCW, two well-established non-linear kinetic models, namely the pseudo-first-order (PFO, Eq. 6) (Lagergren, 1898) and pseudo-second-order (PSO, Eq. 7) (Ho & McKay, 1999) were employed.

$$q_t = q_e (1 - e^{-K_1 t}) \tag{6}$$

$$q_t = \frac{q_e^2 K_2 t}{(1 + K_2 q_e t)} \tag{7}$$

where:  $q_t$  (mg/g),  $K_1$  (1/min), and  $K_2$  (g/mg min) are the biosorption capacity of the dye at time (min), the rate constant of PFO and PSO biosorption, respectively.

Figure 6(a-b) displays the alignment between the experimental results and the designated models, while Table 2 presents the estimated parameters and

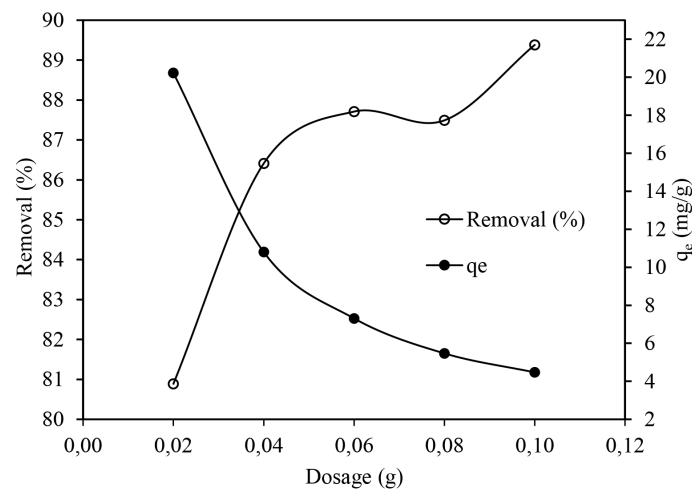
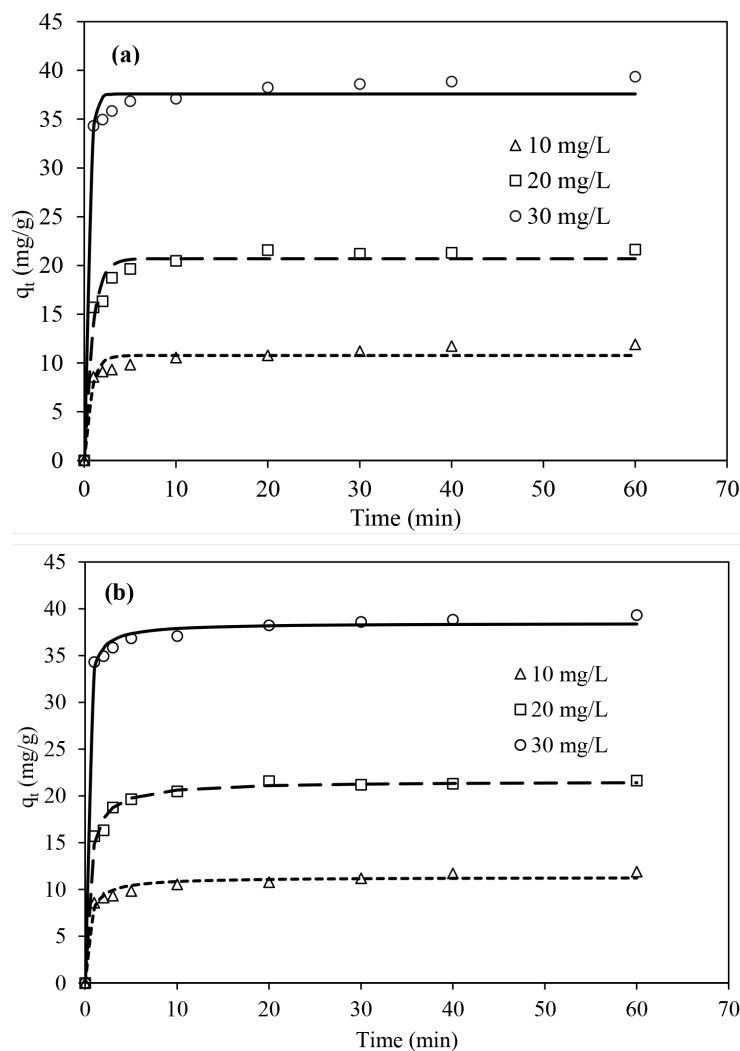


Figure 5. Impact of HPDCW dosage on MG biosorption at an initial concentration of 10 mg/L, pH 9, 300 rpm, and 29 °C



**Figure 6.** Non-linear fitting of (a) PFO and (b) PSO aimed at the MG biosorption kinetic on HPDCW surface on different initial MG concentrations, pH 9, 300 rpm, and 29°C

statistical constants. Based on the analysis of the results, the non-linear PSO is the most appropriate for describing the MG kinetics biosorption on the HPDCW biosorbent. This is because it exhibited a high  $R^2$  value and a lower  $\chi^2$  value compared to the non-linear PFO model. The HPDCW biosorption capacity increased from 11.30 to 21.57 and 38.47 mg/g, as the concentration of MG dye improved from 10 to 20 and 30 mg/L, respectively. This phenomenon can be explained by the observation that elevated concentrations of MG molecules exert a more potent force, enabling them to surpass the obstacle of mass transfer between the biosorbent and the liquid (Hanafiah et al., 2022). Consistent results were noted in other investigations (Lemos et al., 2023; Nguyen et al., 2022).

### Biosorption isotherm studies

Biosorption isotherms display an essential character in optimising the efficiency of

biosorbents as they elucidate the association between the biosorbent and the adsorbate. The shape of an isotherm provides valuable insights into the affinity of molecules for biosorption and the stability of the contacts between the adsorbate and the biosorbent. Various mathematical approaches are employed to characterise biosorption isotherms, ranging from simplified physical models that offer a conceptual understanding of biosorption to empirical methods that necessitate the correlation of results (Musah et al., 2022). The investigation of biosorption isotherms involved varying initial MG concentrations ranging from 10 to 200 mg/L though keeping other experimental conditions constant, such as the biosorbent dose of 0.02 g, agitation speed of 300 rpm, contact period of 60 min and pH of 9. The biosorption behaviour of adsorbates onto a biosorbent was commonly analysed using nonlinear biosorption isotherm models such as Langmuir and Freundlich. However, in the current

**Table 2.** Non-linear PFO and PSO kinetic models aimed at the MG biosorption onto HPDCW biosorbent

MG (mg/L)	$q_{e^{*}exp}$ (mg/g)	PFO				PSO			
		$q_{e^{*}cal}$ (mg/g)	$K_1$ (min <sup>-1</sup> )	$R^2$	$\chi^2$	$q_{e^{*}cal}$ (mg/g)	$K_2$ (g/mg·min)	$R^2$	$\chi^2$
10	11.90	10.77	1.30	0.46	0.59	11.30	0.21	0.82	0.21
20	21.63	20.69	1.11	0.69	0.71	21.57	0.10	0.94	0.16
30	39.35	37.59	2.29	0.41	0.41	38.47	0.17	1.00	0.12

study, neither the Freundlich nor the Langmuir isotherm models sufficiently defined the observed behaviour. The biosorption isotherm plot (Figure 7) displayed a distinct step-like pattern. The form of the biosorption isotherm curve can offer insights into the contact between the adsorbate and the biosorbent. The hypothesis obtained is that the observed steps in the isotherms indicate an uneven distribution of energetic places on the biosorbent surface and the occurrence of physical adsorption. These energetic places may exhibit varying degrees of activity, with some being more active and becoming saturated even at lower concentrations. Furthermore, considering the diverse functional groups of the MG molecules, weak intermolecular interactions between adsorbates may occur in both solution and biosorbent surfaces.

### Comparison of HPDCW performance with other reported biosorbents

So as to verify the efficiency of the current HPDCW biosorbent, its ability to adsorb MG was compared to that of other biosorbents previously mentioned in Table 3. Several biosorbents, including CSC, SAC, SHAC, PAC, BCA, AWCN, and CSAC, exhibited notably reduced performances ranging from 21.51 to 81.00 mg/g. However,

HPDCW demonstrated considerably faster biosorption of MG from the liquid phase, achieving 211.8 mg/g after a mere 5 min. HPDCW showed superior performance compared with other biosorbents, making it an appropriate alternative aimed at extracting low quantities of MG from aqueous solutions.

### Desorption study

Disposing of the used biosorbent could potentially create an additional environmental problem. Therefore, we utilised neutral (distilled water) and acidic media (HCl solutions with concentrations of 0.01 M and 0.02 M) to investigate the removal of MG from HPDCW. The desorption percentage values are low for all the eluents under investigation. Nevertheless, the eluent containing a concentration of 0.02 M HCl had the highest efficiency in recovering the desired substance, resulting in a recovery rate of 16.40%, possibly due to the ion-exchange reaction (Table 4). The contact between MG and HPDCW probably was not just based on electrostatic forces but also involved other weak interactions, which include hydrogen bonding and  $\pi$ - $\pi$  interaction, which were not influenced by variations in ionic strength (El Khomri et al., 2022).

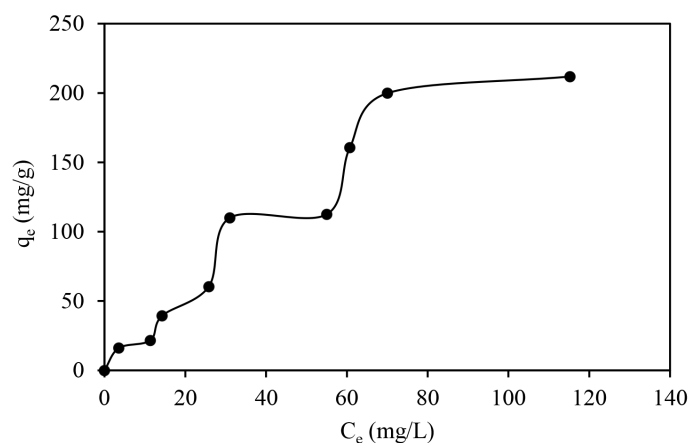


**Figure 7.** Step-like isotherm model of biosorption of MG onto HPDCW at diverse MG concentrations, pH 9, 60 min, and 29 °C

**Table 3.** Valuation of HPDCW biosorption capacities for MG by other reported biosorbents

Biosorbent	Optimum experimental biosorption conditions					$q_{max}$ (mg/g)	References
	Initial MG concentration (mg/L)	Contact time (min)	pH	Temp. (°C)	Biosorbent dosage (g)		
HPDCW	10-200	5	9.0	29	0.02	211.8	This study
Grape stalk	25-300	120	5.0	25	0.8 g/L	214.0	(Lemos et al., 2023)
PLB	1-70	80	8.0	28	0.2 g/L	266.8	(Jabar et al., 2023)
CSC	20–80	225	7.0	25	4 g/L	54.35	(Piriya et al., 2023)
SAC						21.51	
SHAC						22.17	
PAC						32.79	
PAOPT	40–200	20	6.0	25	0.02	217.23	(Zainon et al., 2023)
BCA	50-600	20	6.5	25	0.02	81.00	(Phan et al., 2023)
AWCN	10-60	20	6.6	21	0.10	45.45	(Qaiyum et al., 2022)
CSAC	10–50	420	6.5	30	0.10	61.83	(Azaman et al., 2018)

CSAC: Coconut shell activated carbon, PLB: Plantain leaf biochar, CSC: Coconut shell carbon, SAC: Sulphuric acid-activated carbon, SHAC: Sulphuric acid and hydrogen peroxide solution-activated carbon, PAC: Phosphoric acid-activated carbon, AWCN: Alkali-modified shells of water chestnut, PAOPT: Phosphoric acid-treated oil palm trunk, BCA: Bacteria cellulose-based aerogel.

**Table 4.** The biosorption-desorption ratio by means of distilled water and HCl of 0.01 and 0.02 M at MG concentration of 10 mg/L

Biosorption			Desorption		
[MG] <sub>i</sub> (mg/L)	[MG] adsorbed (mg/L)	Biosorption (%)	Eluent	[MG] <sub>f</sub> (mg/L)	Desorption (%)
3.17	6.83	68.31	Distilled water	0.79	11.58
3.59	6.41	64.10	0.01 M HCl	0.93	14.51
3.61	6.39	63.90	0.02 M HCl	1.05	16.40

## CONCLUSIONS

Desiccated coconut waste was subjected to chemical treatment using 15% (v/v) of H<sub>2</sub>O<sub>2</sub>. The resulting product, referred to as HPDCW, was utilised as a cost-effective biosorbent to remove MG, an example of a hazardous cationic dye. According to the analysis using FTIR, SEM-EDX, and isotherm tests, it has been determined that the HPDCW has a beneficial impact on MG biosorption. This is primarily owing to the existence of a rough surface and functional groups such as carboxylic acid, amino and hydroxyl on HPDCW. The optimal parameters for MG biosorption using HPDCW include a dosage of 0.02 g, a pH of at least 7, and only 5 min contact time. The analysis of the kinetics revealed that the process of MG biosorption adhered to a PSO model. The results obtained from the isotherm and desorption tests indicated the potential occurrence of  $\pi$ - $\pi$  stacking contact, hydrogen bonding, and electrostatic attraction amongst the MG molecules and HPDCW surface. Due to the high value of maximum biosorption capacity and fast MG uptake, the biosorbent material is cheap, and the pretreatment process is easy; HPDCW can become an alternative biosorbent for eliminating MG from aqueous media.

## REFERENCES

- Al-Amrani, W.A., Hanafah, M.A.K.M., Mohammed, A.A. 2022. A comprehensive review of anionic azo dyes adsorption on surface-functionalised silicas. *Environmental Science and Pollution Research*, 29, 76565-76610
- Azaman, S.A.H., Afandi, A., Hameed, B.H., Din, A.T.M. 2018. Removal of malachite green from aqueous phase using coconut shell activated carbon: Adsorption, desorption, and reusability studies. *Journal of Applied Science and Engineering*, 21(3), 317–330.
- Bello, O.S., Ahmad, M.A. 2012. Coconut (*Cocos nucifera*) shell based activated carbon for the removal of malachite green dye from aqueous solutions. *Separation Science and Technology*, 47(6), 903–912.
- Chong, M.Y., Tam, Y.J. 2020. Bioremediation of dyes using coconut parts via adsorption: a review. *SN Applied Sciences*, 2(187).
- El Khomri, M., El Messaoudi, N., Dbik, A., Bentahar, S., Lacherai, A., Faska, N., Jada, A. 2022. Regeneration of argan nutshell and almond shell using HNO<sub>3</sub> for their reusability to remove cationic dye from aqueous solution. *Chemical Engineering Communications*, 209(10), 1304–1315.
- Ganiyu, S.A., Suleiman, M.A., Al-Amrani, W.A., Usman, A.K., Onaizi, S.A. 2023. Adsorptive removal

- of organic pollutants from contaminated waters using zeolitic imidazolate framework Composites: A comprehensive and Up-to-date review. *Separation and Purification Technology*, 318, 123765.
7. Hanafiah, M.A.K.M., Bakar, N.A.A., Al-Amrani, W.A., Ibrahim, S., Malek, N.A.N.N., Jawad, A. H. 2022. Preparation, characterization and application of sulphuric acid-treated soursop (*Annona muricata* L.) seeds powder in the adsorption of Cu(II) ions. *Nature Environment and Pollution Technology*, 21(1), 217–223.
  8. He, J., Mo, P., Luo, Y.-S., Yang, P.-H. 2023. Strategies for solving the issue of malachite green residues in aquatic products: a review. *Aquaculture Research*, 2023, 8578570.
  9. Ho, Y.S., McKay, G. 1999. Pseudo-second order model for sorption processes. *Process Biochemistry*, 34(5), 451–465.
  10. Jabar, J.M., Adebayo, M.A., Odusote, Y.A., Yilmaz, M., Rangabhashiyam, S. 2023. Valorization of microwave-assisted H<sub>3</sub>PO<sub>4</sub>-activated plantain (*Musa paradisiacal* L) leaf biochar for malachite green sequestration: models and mechanism of adsorption. *Results in Engineering*, 18, 101129.
  11. Khalid, K., Hanafiah, M.A.K., Al-Amrani, W.A., Malek, N.A.N., Fatinathan, S. 2022. Comparative adsorption of methylene blue dye on hexane-washed and xanthated spent grated coconut (*Cocos nucifera* L.): Isotherms, thermodynamics and mechanisms. *Journal of Ecological Engineering*, 23(3), 1–11.
  12. Lagergren, S.K. 1898. About the theory of so-called adsorption of soluble substances. *Sven Vetenskapssakad Handlingar*, 24, 1–39.
  13. Lemos, E.S., Fiorentini, E.F., Bonilla-Petriciolet, A., Escudero, L. B. 2023. Malachite green removal by grape stalks biosorption from natural waters and effluents. *Adsorption Science & Technology*, 2023, 6695937.
  14. Musah, M., Azeh, Y., Mathew, J.T., Umar, M.T., Abdulhamid, Z., Muhammad, A.I. 2022. Adsorption kinetics and isotherm models: a review. *CaJoST*, 4(1), 20–26.
  15. Nguyen, P.X.T., Ho, K.H., Do, N.H.N., Nguyen, C.T.X., Nguyen, H.M., Tran, K.A., Le, K.A., Le, P.K. 2022. A comparative study on modification of aerogel-based biosorbents from coconut fibers for treatment of dye- and oil-contaminated water. *Materials Today Sustainability*, 19, 100175.
  16. Phan, H.T., Nguyen, K.D., Nguyen, H.H.M., Dao, N.T., Le, P.T.K., Le, H.V. 2023. Nata de coco as an abundant bacterial cellulose resource to prepare aerogels for the removal of organic dyes in water. *Bioresource Technology Reports*, 24, 101613.
  17. Piriya, R.S., Jayabalakrishnan, R.M., Maheswari, M., Boomiraj, K., Oumabady, S. 2023. Comparative adsorption study of malachite green dye on acid-activated carbon. *International Journal of Environmental Analytical Chemistry*, 103(1), 16–30.
  18. Prasad, B., Mishra, A., Goswami, R. 2023. Malachite green dye adsorption using activated pine ash. *AIP Conference Proceedings*, 2521(1).
  19. Qaiyum, M.A., Mohanta, J., Kumari, R., Samal, P.P., Dey, B., Dey, S. 2022. Alkali treated water chestnut (*Trapa natans* L.) shells as a promising phytosorbent for malachite green removal from water. *International Journal of Phytoremediation*, 24(8), 822–830.
  20. Revellame, E.D., Fortela, D.L., Sharp, W., Hernandez, R., Zappi, M.E. 2020. Adsorption kinetic modeling using pseudo-first order and pseudo-second order rate laws: A review. *Cleaner Engineering and Technology*, 1, 100032.
  21. Saikia, H., Brahma, D., Nath, H., Borah, D., Deb-nath, M. 2022. Coconut husk ash fabricated CoAl-layered double hydroxide composite for the enhanced sorption of malachite green dye: isotherm, kinetics and thermodynamic studies. *Inorganic Chemistry Communications*, 144, 109878.
  22. Somsiripan, T., Sangwichien, C. 2023. Enhancement of adsorption capacity of methylene blue, malachite green, and rhodamine B onto KOH activated carbon derived from oil palm empty fruit bunches. *Arabian Journal of Chemistry*, 16(12), 105270.
  23. Song, C., Gao, C., Fatehi, P., Wang, S., Jiang, C., Kong, F. 2023. Influence of structure and functional group of modified kraft lignin on adsorption behavior of dye. *International Journal of Biological Macromolecules*, 240, 124368.
  24. Umeh, C.T., Akinyele, A.B., Okoye, N. H., Emmanuel, S.S., Iwuozor, K.O., Oyekunle, I.P., Ocheje, J.O., Ighalo, J.O. 2023. Recent approach in the application of nano-adsorbents for malachite green (MG) dye uptake from contaminated water: A critical review. *Environmental Nanotechnology, Monitoring & Management*, 20, 100891.
  25. Widiartayasa Prihatdini, R., Suratman, A., Siswanta, D. 2023. Linear and nonlinear modeling of kinetics and isotherm of malachite green dye adsorption to trimellitic-modified pineapple peel. *Materials Today: Proceedings*, 88, 33–40.
  26. Zainon, A.Z.A., Al-Amrani, W.A., Mohd, S.F.B., Ibrahim, S., Megat Hanafiah, M.A.K. 2023. Phosphoric acid treated oil palm trunk waste for removal of malachite green—kinetics and isotherm investigations. *Ecological Engineering & Environmental Technology*, 24, 33–43.
  27. Zhang, Y., Zheng, Y., Yang, Y., Huang, J., Zimmerman, A.R., Chen, H., Hu, X., Gao, B. 2021. Mechanisms and adsorption capacities of hydrogen peroxide modified ball milled biochar for the removal of methylene blue from aqueous solutions. *Bioresource Technology*, 337, 125432.